

# Monitoring fatigue damage of an adhesive joint using fiber optics sensors

C S Shin<sup>1,3</sup>, Y J Yang<sup>1</sup> and S K Liaw<sup>2</sup>

<sup>1</sup>Mechanical Engineering, National Taiwan University, No.1, Sec.4, Roosevelt Road, Taipei, 10617, Taiwan, (R.O.C.)

<sup>2</sup>Electronic and computer engineering, National Taiwan Univ of Science and Technology, Taipei, Taiwan, No.43, Sec. 4, Keelung Rd., Taipei 106, Taiwan (R.O.C.)

<sup>3</sup> Author to whom any correspondence should be addressed (csshin@ntu.edu.tw).

**Abstract.** Adhesive joining has many merits over traditional joining techniques. However, adhesive joints are susceptible to damage and degradation caused by service loading. If such degradation went undetected, serious structural failures and catastrophic outcome might follow. It is difficult and economically unviable to carry out regular examination on the joint integrity using conventional non-destructive evaluation techniques, especially in the case of practical structures with large scale adhesive joining. In this work, optical fibers with Bragg grating (FBG) sensors embedded in single lap joints has been demonstrated to be able to detect internal damage caused by monotonic and cyclic loading. FBG sensor works by reflecting specific wavelengths from a broad spectrum incident light. The wavelengths reflected depend on the strain on the FBG. Internal damages will perturb the strain field in the joint and thus change the shape of the reflected FBG spectrum. With embedded FBG sensors, it is possible to achieve on-line monitoring of the joint integrity in an economical way.

## 1. Introduction

Traditional joining using bolts or rivets requires stress concentrating holes to be drilled in a structure. Joining by welding may degrade the materials in the heat affected zone. These shortcomings may be overcome by using adhesive joining [1-3]. The availability of adhesive joints also allows light alloys and fiber reinforced composites structures to overcome the problems of weak out-of-plane bending strength/stiffness, low joint toughness while improving their crash-worthiness associated with traditional joining. However, occasional overloading and fluctuating service loading may degrade these joints. If such degradation went undetected, serious structural failures and catastrophic outcome might follow.

Non-destructive examination (NDE) techniques such as ultrasonic scan are commonly used to examine the integrity of adhesive joints [4-9] and neutron irradiation was found to be more effective than ultrasonic to detect internal damages in a joint [9]. The use of thermography [10] and shearography [11] has also been proposed. Current NDE techniques can detect debonding readily but cannot reliably detect all internal defects and degradation of an adhesive joint [12, 13]. For example, a kissing joint that has full interfacial contact but does not possess the required structural strength is difficult to detect using the current techniques [14]. Moreover, It is economically unviable to carry out regular examination of the joint integrity using traditional NDE techniques, especially in structures



with large scale adhesive joining. On the other hand, strain gages had been employed for monitoring the integrity of the joint in an adhesive patch repair. The latter method not only allows continuous monitoring but also is much more economical than periodic examination of the whole bonded region using ultrasonic techniques [15]. However, as strain gages can only be applied to the outer surface, they are susceptible to environmental degradation and may not possess sufficient fatigue life for long term monitoring [15]. Optical fiber sensors are known to have much better fatigue strength. They can be embedded inside the bond and relatively free from environmental attack. The feasibility of using fiber Bragg grating (FBG) sensors for monitoring has been investigated in this work.

## 2. Material and methods

### 2.1. Fiber Bragg Grating sensor and its basic properties

When a broadband light is coupled into an optical fiber with a uniform Bragg grating, a single peak with wavelength  $\lambda$  satisfying the Bragg diffraction criterion will be reflected:

$$\lambda = 2n_e\Lambda \quad (1)$$

where  $n_e$  is the effective refractive index and  $\Lambda$  is the periodicity of the grating. When either or both of the  $n_e$  and  $\Lambda$  change, the center wavelength of the reflected spectrum shifts.  $\Lambda$  will be changed if the FBG is subjected to a deformation. Such deformation may be caused by mechanical or thermal strains.  $n_e$  will be affected by variation in temperature and the triaxial stress state acting on the fiber. If the FBG is subjected to a non-uniform strain field, uniformity of the grating period is perturbed, the single peak reflected spectrum will broaden or chirped. In general, the reflected wavelength will shift by  $\sim 1\text{pm}$  under a strain of  $1\ \mu\epsilon$  or a temperature change of  $0.1^\circ\text{C}$ . If temperature variation is negligible, the change in the spectrum basically reflects a change in the stress/strain status along the FBG.

FBGs used were fabricated in a Ge–B co-doped single mode fiber by side writing using a phase mask with a period of  $1.05\ \mu\text{m}$ . The sensing length of the FBGs was about 10 mm. The reflectivity of the resulting FBG was about 99%, and the peak wavelengths were between 1545 and 1547nm. The FWHM (full width half maximum) of the FBGs was about 0.175 nm. The reflected spectra from the FBGs were interrogated using an optical spectrum analyzer (Anritsu MS9710C OSA).

### 2.2. Single lap joint specimens

6061-T6 aluminum strips were glued together with Loctite E-30CL structural epoxy adhesive to forms single lap joint specimens (Fig.1). Optical fibers with FBG are embedded at either  $0^\circ$  (parallel to loading direction),  $45^\circ$  or  $90^\circ$  in the lap joint as shown schematically in Fig.2. The sensor designation

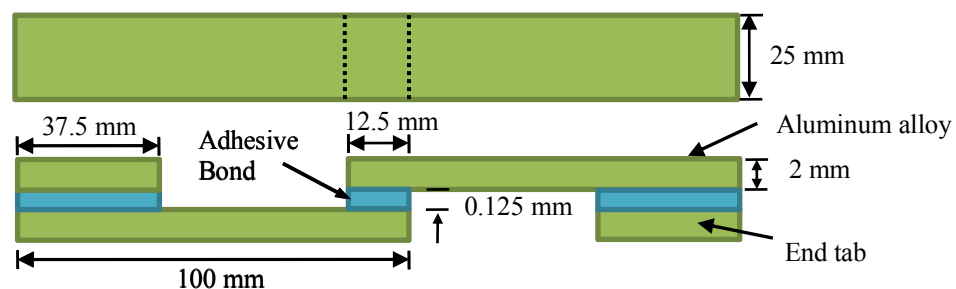


Fig.1 Dimensions of the single lap joint specimen.

is in the form  $DnPx$ , where  $n$  represents the orientation angle and  $x$  denotes the location.  $x$  may take the letter E (edge), L(left), M(middle) or R(right). The relative positions of these locations are indicated in Fig.2. The bond line is approximately as thick as the diameter of the optical fiber, i.e. 125  $\mu\text{m}$ . The specimens were subjected to tensile or cyclic loading. Testings were interrupted periodically to allow the reflected light spectra from the FBGs to be recorded at the instantaneous loading and at 0 N. These spectra were compared with the respective original spectra before testing. The recorded spectra covered a span of 10 nm to ensure the characteristic FBG wavelength was totally included. For each set of testing conditions, the tests have been repeated at least three times to ensure the results are consistently reproducible.

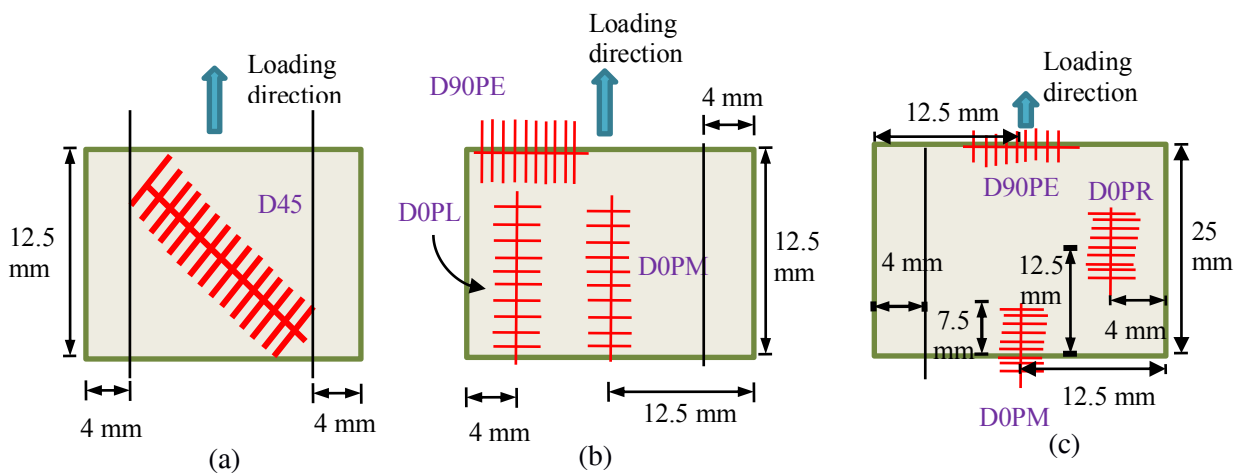


Fig.2 Different layouts of the FBG sensors in the adhesive bond.

### 3. Results and discussion

#### 3.1. Damage monitoring during tensile tests

*3.1.1. Sensitivities of different FBG orientations in response to damage under tensile tests.* Fig.3 shows the spectrum from the 45° FBG configuration (Fig.2a) under different loading. As the applied tensile loading on the specimen increased, the FBG spectra initial shifted to the longer wavelength and eventually chirped and changed shape significantly. The reflected wavelengths from an FBG are affected by the strain acting on the FBG. The presence of internal damages will perturb the strain field in the joint and thus change the shape of the reflected FBG spectrum. On the other hand, loading the specimen will stress the joint and cause a wavelength shift of the spectrum. Non-uniform strain induced by stress concentration near the edges of the joint will chirp or even split the spectrum. To differentiate spectrum change caused by damage from the latter effects, spectra were recorded with the specimens fully unloaded after loading to different levels.

On unloading from 90% of failure load, the FBG spectrum started to show slight change in shape (Fig.3b), suggesting the existence of internal damages in the adhesive bond at this load level. Damage became more intensive on loading up to 95% of failure load and thus induced a more significant change in the FBG spectrum on unloading (Fig.3c).

Fig. 4 shows the spectrum from the 0° and 90° FBG configurations (Fig.2b) under different loading. For the 0° FBGs, the spectra changed shapes much more heavily (Figs. 4a & b) than the 45° FBG under similar loading. On the other hand, spectra from the 90° FBG changed very little shape even near failure (Fig. 4c). The same trends occur in the unloading spectra (Figs. 4d-f). As a result, it may

be concluded that the  $0^\circ$  FBG is the most sensitive to damage inside the bond and the  $90^\circ$  FBG is the least sensitive while the sensitivity of the  $45^\circ$  FBG lies in between.

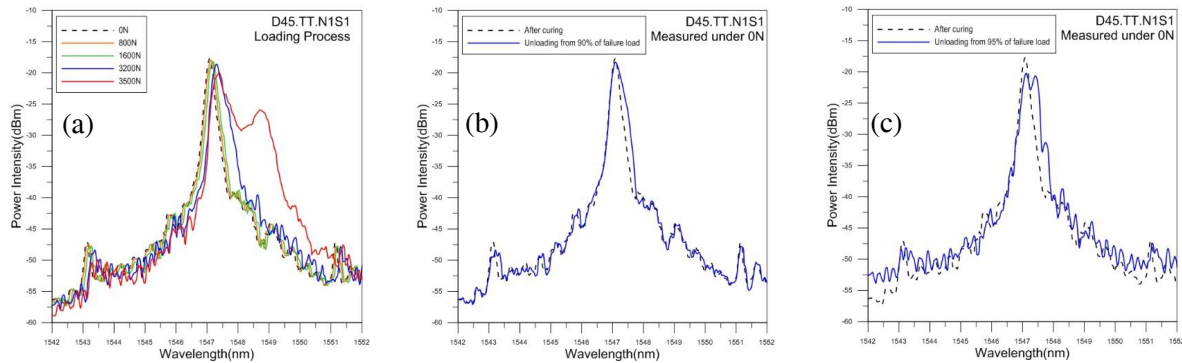


Fig.3 Spectrum measured from the  $45^\circ$  FBG under various loading.

The D0PM unloading spectrum from 87% of failure load (Fig. 4e) showed slightly more well-defined changes than that from D0PL. Results from two other specimens tested under the same conditions also exhibited the same phenomenon. This suggests that the  $0^\circ$  FBG located in the middle of the bond (D0PM) is slightly more sensitive than the one located on the left (D0PL). This may be due to damages started to occur earlier in the middle.

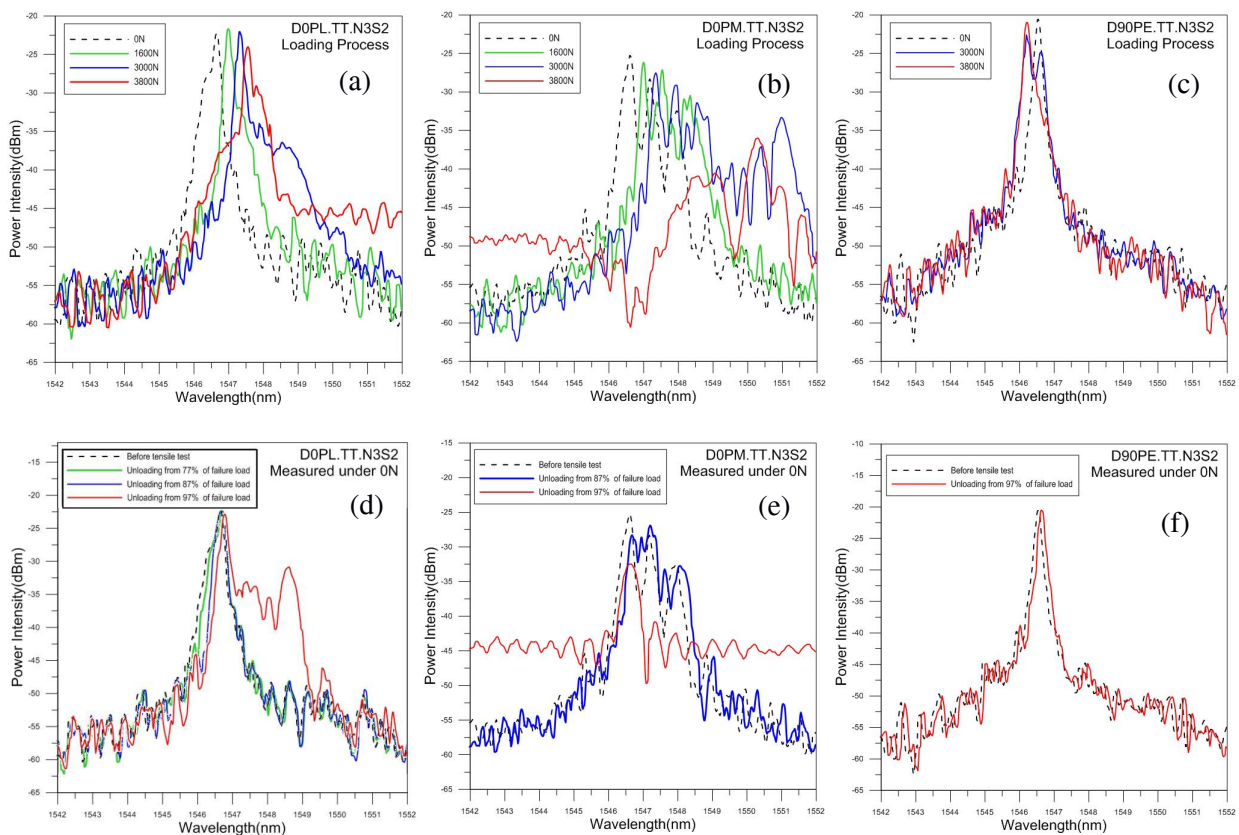


Fig.4 Spectra measured from the  $0^\circ$  and  $90^\circ$  FBGs under various loading.

**3.1.2. Effect of of FBG locations on sensitivities in response to damage.** It is known that stress concentration occurs near the edges where the adhesive bond lines end in the loading direction. Since the sensing length of the FBG employed was about 10mm and there was likely a  $\pm 1$ mm deviation in positioning it in the bond, the  $0^\circ$  FBGs in configuration depicted in Fig.2b may or may not touch the ending edges of the bond. To investigate the difference in sensing sensitivity when the  $0^\circ$  FBG covers the edge of the bond or well clear of it, a joint overlapping length of 25mm instead of 12.5mm was used. The D0PM FBG was deliberately placed across one edge so that 2.5mm of it was outside the bond. On the other hand, the D0PL FBG was placed in the center of the bond so that it was about 7.5mm from either bond edges. As results above suggest that damages may start earlier in the middle, a  $90^\circ$  FBG (D90PE) was also included and was placed very close to the edge and centered in the middle instead of on the left. The complete lay out is shown schematically in Fig.2c.

Fig.5 shows the unloading spectra from each FBG after loading up to various loads. The unloading spectra from the  $90^\circ$  FBG and the  $0^\circ$  FBG well inside the bond showed virtually no change up to 95% of the failure load. The one straddling one bond edge (D0PM) started to show marked change in the unloading spectra at 84% of the failure load. This shows clearly  $0^\circ$  FBGs in the vicinity of the ending edges of an adhesive bond has much greater sensitivity than FBG well clear of the edge.

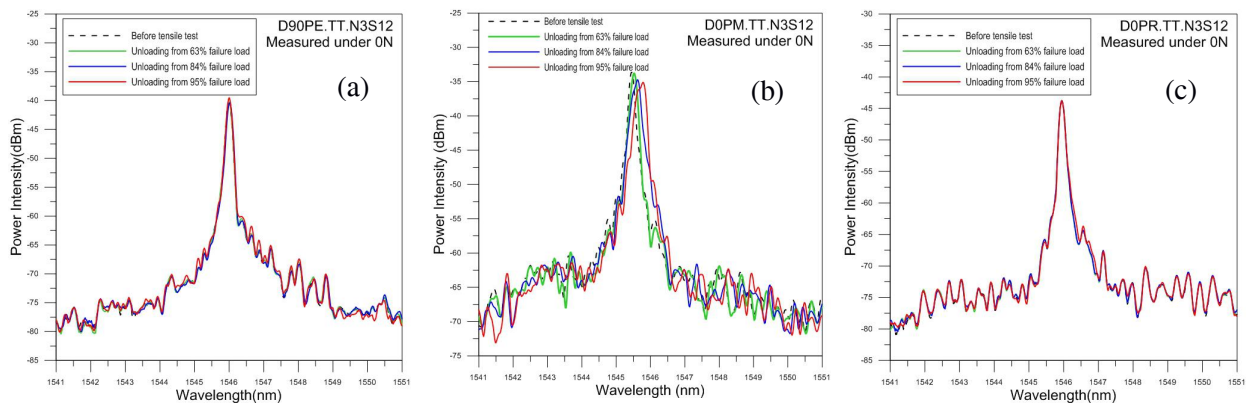


Fig.5 Unloading spectra measured from the  $0^\circ$  and  $90^\circ$  FBGs using the configuration in Fig.2(c).

### 3.2. Damage monitoring under fatigue tests

In these tests, the lap joints were 12.5mm in length. FBG layout was similar to Fig.2b except that the  $90^\circ$  FBG was changed to  $0^\circ$  and was placed 4mm from the right side. Also the center of the FBGs were positioned at the transverse center line of the bond as far as possible so that their ends were within 1.5mm from either ending edge of the bond. The specimens were cycled between 0.156kN and 1.56kN at a frequency of 5Hz. The minimum and maximum loads corresponds to 4% and 40% of the average tensile failure load. The resulting average fatigue life was 144860 cycles.

**3.2.1. Virgin specimens fatigue testing.** Fig.6 shows the unloading spectra from the three FBGs near the end of fatigue life. For the D0PL FBG, no marked change in the shape of the spectrum occurred up to 125000 cycles (95% life). At 130000 cycles (98% life), a prominent rise in background intensity was observed (Fig.6a). The D0PM spectra started to show discernible change at 115000 cycles, or 87% life (Fig.6b). The spectra continued to evolve and at 130000 cycles, it differed quite significantly from the initial spectrum (Fig.6c). The D0PR spectra started to show slight change at 95000 cycles (72% life). The change became quite marked at 115000 cycles (Fig.6d) and 130000 cycles (Fig.6e).

Fatigue damage is a highly localized and stochastic in nature. After damage initiated, it develops slowly under the small cyclic loading and may only affect the FBG in its vicinity. This explains why some FBG showed spectrum change much earlier and more significantly than the others.

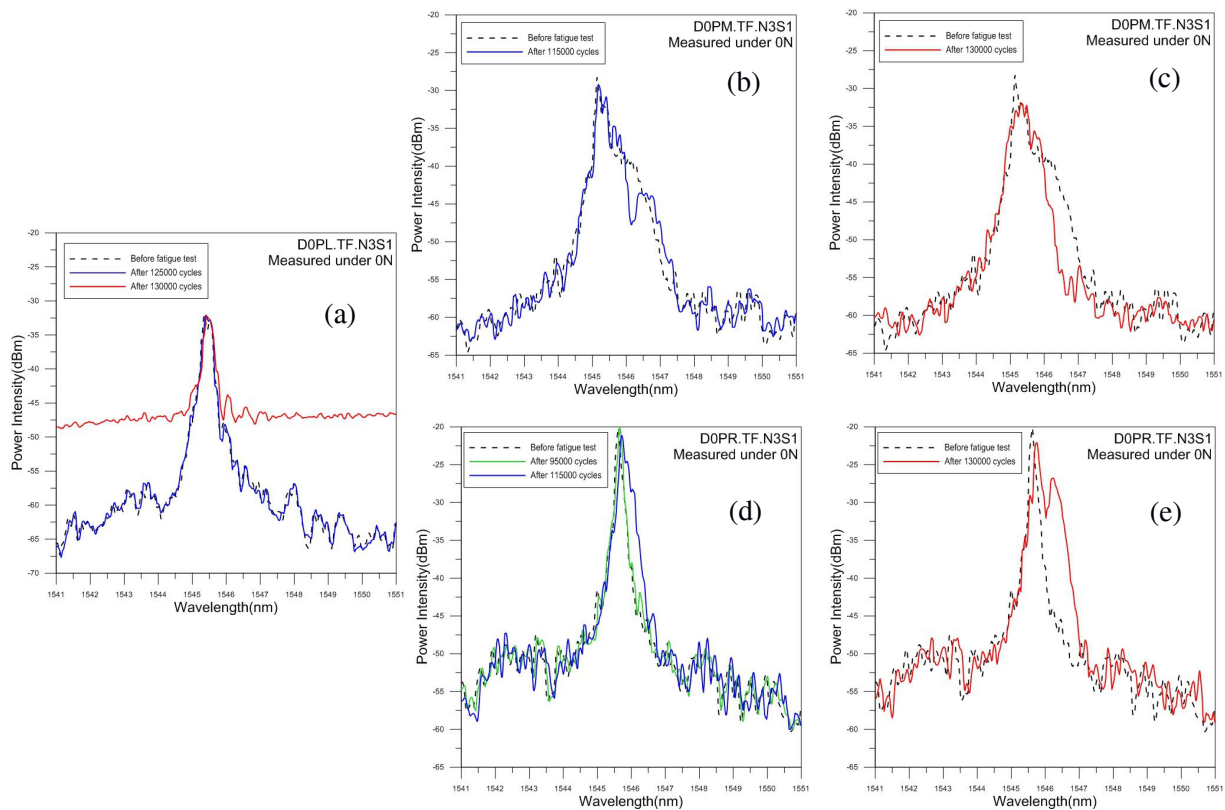


Fig.6 Unloading spectra from the three  $0^\circ$  FBGs near the end of fatigue life.

**3.2.2. Pre-tensioned specimens fatigue testing.** Tensile loading was applied to two batches of specimens. In the first batch, applied loading was increased stepwise until the unloading spectra of all three  $0^\circ$  FBG started to show discernible changes. In the second batch, stepwise increase of the applied loading was just stopped short of causing discernible change in the unloading spectra. Fig.7 shows the spectra of one specimen in the first batch unloaded from a maximum load of 2500 N, which corresponds to about 63% of the average tensile failure loading. On fatigue cycled between 0.156kN and 1.56kN, it got a life of 34600 cycles, significantly shorter than the average life of 144860 cycles.

A specimen in the second batch was loaded to 2000N, which corresponded to about 50% of the average tensile failure loading and was higher than the maximum cyclic loading of 1560N. The unloading spectra from all three  $0^\circ$  FBG showed no discernible changes. Follow up fatigue test gave a life of 137250 cycles, which is within the scatter of the virgin specimen fatigue life.

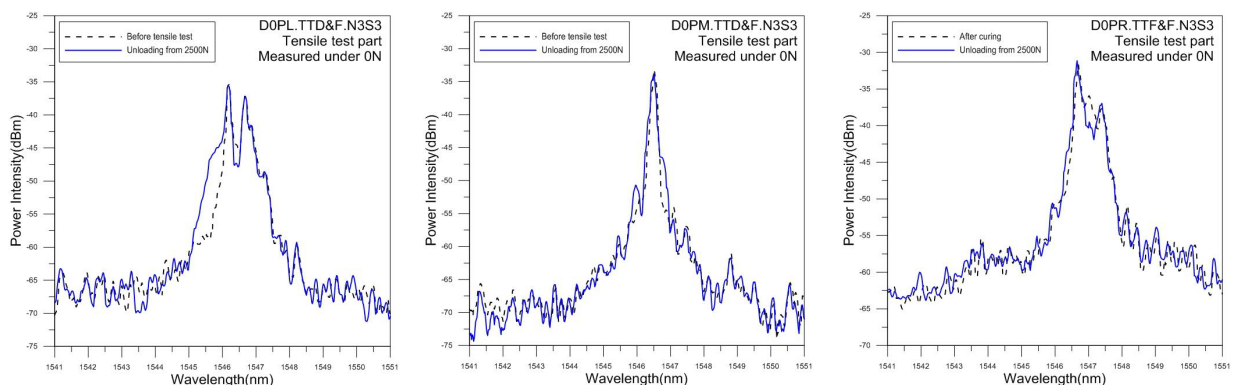


Fig.7 Unloading spectra from the three  $0^\circ$  FBGs which just started to show discernible changes.

#### 4. Conclusions

FBG sensor embedded in an adhesive bond is able to detect the occurrence of internal bond damages due to tensile and fatigue loading and the signal is exhibited as a change in shape of its reflected spectrum under the load free condition. A 0° FBG aligning with the loading direction is more sensitive to bond damage detection than a 45° one. A 90° FBG is the least sensitive among the three. The 0° FBG detects bond damage sooner when it is straddling the ending edge of of the bond than when it is well clear of the edges. When the unloading spectra from a 0° FBG in a pre-tensioned specimen showed discernible change in shape, its fatigue life is significantly reduced when compared with the one that has not yet showed discernible change.

#### References

- [1] da Silva L F M, Öchsner A. and Adams R D 2011 *Handbook of Adhesion Technology* (Berlin Heidelberg: Springer)
- [2] Banea M D and da Silva L F M 2009 *J. Mater. Des. Appl.* **223** 1-18.
- [3] Adams R D, Comyn J. and Wake W C 1997 *Structural adhesive joints in engineering 2nd ed.* (London: Chapman & Hall)
- [4] Allin J M 2002 *Disbond detection in adhesive joints using low frequency ultrasound* PhD thesis, Mech. Engng. Imperial College London
- [5] Amami S, Santos S D, Savin A, Jeong W J, Bae J H, Joh K H and Ha M K 2010 Société Française d'Acoustique - SFA. *10ème Congrès Français d'Acoustique* (Lyon France)
- [6] Hemantha L M and Mallika M S L R 2013 *Int. J. Engng. Research & Technology*, **2(1)**
- [7] Zhang H 2013 *J. Appl. Sci.* 13 (**22**) 5298-5308
- [8] Elgharib E E, Abdelhay A M and Etman M I 2013 *Int. J. Engng. Res. & Tech.* **2(12)**
- [9] Michaloudaki M 2005 *An Approach to Quality Assurance of Structural Adhesive Joints* (Munich: Techn. Univ.) PhD Thesis
- [10] Meola C, Bruzzone A, Giorleo L, Morace R E and Vitiello A. 2004 *J. Adhesion Sci. Tech.* **18** 635-654.
- [11] Hung M Y Y, Chen Y S, Ng S P, Shepard S M, Hou Y and Lhota J L 2007 *Op. Engng.* **46 (5)** 051007
- [12] Roach D, Rackow K and Duvall R 2010 *Proc. 10th Eur. Conf. on Non-Destructive Testing* (Moscow, Russia) **5** 3263
- [13] Kalms M, Hellmers S, Huke P and Bergmann R B 2014 *Proc. SPIE 9063, Nondestructive Characterization for Composite Materials, Aerospace Engineering, Civil Infrastructure, and Homeland Security* (San Diego, California, USA) 906327
- [14] Yan D, Drinkwater B W and Neild S A 2009 *NDT&E International* **42** 459-466
- [15] Baker A A 2008 *Structural Health Monitoring of a Bonded Composite Patch Repair on a Fatigue-Cracked F-111C Wing* Australia DSTO-RR-0335

#### Acknowledgement

The authors would like to thank the Ministry of Science and Technology, ROC for funding this work through the project MOST 104-2221-E-002 -036 -MY3.